LANGMUIR

pubs.acs.org/Langmuir Article

Multichannel Multijunction Droplet Microfluidic Device to Synthesize Hydrogel Microcapsules with Different Core−Shell Structures and Adjustable Core Positions

Qiong Wu,[¶] Xing Huang,[¶] Ran Liu, Xinzhu Yang, Gao Xiao, Nan Jiang, David A. Weitz, and Yujun Song*

Cite This: https://doi.org/10.1021/acs.langmuir.3c02579 Read Online

ABSTRACT: Core−shell hydrogel microcapsules have sparked great interest due to their unique characteristics and prospective applications in the medical, pharmaceutical, and cosmetic fields. However, complex synthetic procedures and expensive costs have limited their practical application. Herein, we designed and prepared several multichannel and multijunctional droplet microfluidic devices based on soft lithography for the effective synthesis of core−shell hydrogel microcapsules for different purposes. Additionally, two different cross-linking processes (ultraviolet (UV) exposure and interfacial polymerization) were used to synthesize different types of core−shell structured hydrogel microcapsules. Hydrogel microcapsules with gelatin methacryloyl (GelMA) as the core and polyacrylamide (PAM) as the thin shell were synthesized using UV cross-linking. Using an interfacial polymerization process, another core−shell structured microcapsule with GelMA as the core and Ca^{2+} cross-linked alginate with polyethylenimine (PEI) as the shell was constructed, and the core diameter and total droplet diameter were flexibly controlled by carving. Noteworthy, these hydrogel microcapsules exhibit stimuli-responsiveness and controlled release ability. Overall, a novel technique was developed to successfully synthesize various hydrogel microcapsules with core−shell microstructures. The hydrogel microcapsules possess a multilayered structure that facilitates the coassembly of cells and drugs, as well as the layered assembly of multiple drugs, to develop synergistic therapeutic regimens. These adaptable and controllable hydrogel microdroplets shall held great promise for multicell or multidrug administration as well as for high-throughput drug screening.

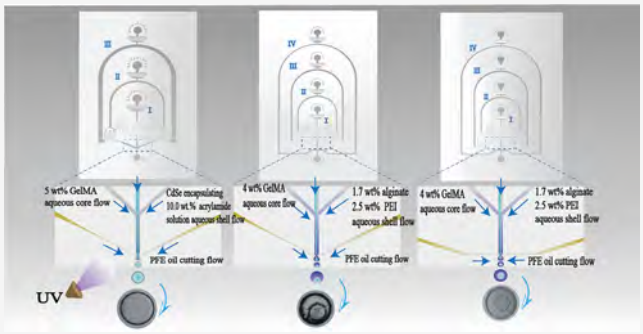

■ INTRODUCTION

Three-dimensional polymer networks, cross-linked chemically or physically and imbibing a large amount of water, are referred to as hydrogels. The multitude of their application in drug loading and delivery,[1] chemical sensors,[2] tissue engineering,[3] and water-holding agents[4,5] has attracted widespread interest in the scientific community. Smart hydrogels are, in particular, one of the most promising materials.[6] Due to the existence of specific functionalities or adjustable cross-links, smart hydrogels in their swollen state can undergo significant changes by absorbing or expelling water in response to changes in their external environment, including ionic strength or pH,[7,8] temperature,[9,10] substrate concentration,[11−13] electric signal and light, etc. Lately, stimuli-responsive hydrogel materials have piqued a great deal of interest in account of their preponderant properties in the field of medicine,[14−16] sensors[17] and chemical separation,[18,19] etc. By virtue of their uniform shape, hydrogel microcapsules have been acknowledged as one of the most promising hydrogel materials.[20−23] Given that researchers may now impart different characteristics to the core and shell to enable flexible functionalization, hydrogel microcapsules with core−shell structures in particular have a bright future in today's more complex applications, such as drug administration.[23]

Microcapsules having core−shell architectures, wherein the active ingredients in the cores are shielded from the outside environment by the shells, have been used in a number of different fields such as foods,[24,25] cosmetics,[26,27] pharmaceutics,[28] printing,[29,30] and self-healing materials.[31,32] Utilizing a variety of solidification processes, including solvent evaporation, ionic cross-linking, and photo or heat polymerization, monodisperse core−shell droplets may be utilized as a

Received: September 1, 2023
Revised: November 7, 2023
Accepted: November 7, 2023

template to create microcapsules.[33] Liquid microcapsules are a significant subclass of core−shell microcapsules having uses in the administration of medications, nutrients, and cells, as well as in the processing of food, cosmetics, and controlled release.[34,35] Polymerization, layer-by-layer adsorption, electrospraying, and spray-drying are a few traditional methods for creating core−shell microcapsules.[36] The potential of the developed particles is, however, constrained by these approaches' poor control over structure, size, and process parameters, excessive material requirements, and poor encapsulation efficiency.[37−42]

It has been demonstrated that droplet microfluidics offers a fresh and promising method for the fabrication of microcapsules.[33,43] With well-controlled flow conditions, microfluidic approaches could overcome the aforementioned difficulties with conventional preparation techniques.[42,44] Core−shell droplets produced by droplet-based microfluidics are homogeneous and highly monodispersed. The droplets thus generated can be controlled further by different means.[42,45] Microfluidic technology simplifies the fabrication of monodisperse core−shell droplets that serve as ideal templates for creating microcapsules using a variety of solidification techniques; these techniques may include photo- or thermally induced free-radical polymerization,[46,47] solvent evaporation,[48] freezing,[49] and ironic cross-linking.[50] To date, multiple-step or one-step droplet formation has been involved in the preparation of core−shell templates. In the multiple-step method, core drops are produced first using multiple T-junctions,[40,51] multiple flow-focusing junctions,[52,53] coflowing junctions,[54] or three-dimensional devices,[55] and subsequently, the shell drops encapsulating these core drops are produced in the continuous phase as a separate step.[33] By carefully regulating the external, intermediate, and internal phase flow rates, this approach can create monodisperse core−shell droplets. Thus, to create hydrogel microcapsules with a core−shell structure, microchannels based on a multistep process were therefore fabricated.

Gelatin methacryloyl (GelMA)-based hydrogels have excellent cell adhesion sites and are biocompatible when used as the cores of core−shell structured microcapsules.[56−58] By replacement of the amine group in gelatin with methacrylate anhydride, gelatin is modified into GelMA anhydride.[59] Gelatin, undoubtedly, is an intriguing polymer owing to the existence of Arg-Gly-Asp (RGD), bioactive sequences that are useful for cell entrapment, and allow active molecular species to undergo binding with the polymeric network.[60,61] Nevertheless, GelMA-based hydrogels have rather poor mechanical characteristics (i.e., toughness and strength).[56]

The weak mechanical qualities of GelMA can be compensated for by the shell of the core−shell structured microcapsules, which are made of polyacrylamide (PAM). Polyacrylamide (PAM) may be classified as a typical synthetic hydrogel with outstanding mechanical characteristics, favorable chemical stability, and a high antipollution capacity.[62−65] Typically, the PAM microspheres are produced using low concentrations of acrylamide (AM) and cross-linkers.[65,66] The polymer sodium alginate (SA) is another intriguing polymeric material. Although a single SA hydrogel has a low mechanical strength and a large affinity for dyes and metal ions due to its numerous hydroxyl and carboxyl groups, cross-linking with Ca^{2+} by chelation can significantly increase the stability of the structure.[67,68] A junction is created when a pair of units of two distinct chains of SA bind to the same calcium ion. An "egg-box" is created as a result of this association, eventually generating a network.[61]

Herein, we designed and prepared several multichannel and multijunctional droplet microfluidic devices based on soft lithography for the effective synthesis of core−shell hydrogel microcapsules for various applications. Meanwhile, two different cross-linking processes (UV exposure and interfacial polymerization) were utilized to synthesize different types of core−shell structured hydrogel microcapsules. A UV-based cross-linking and interfacial polymerization technique was used to fabricate two types of core−shell structured hydrogel microcapsules. Using the fabrication of these microdroplets as a foundation, the geometry of the poly(-dimethylsiloxane) (PDMS) microfluidic device was optimized, and a multistep exposure and mask alignment technique was created to prepare a channel junction with the core channel precisely in the center of the shell channel, placing the core of the core−shell hydrogel droplet in the center. Importantly, these hydrogel microcapsules exhibit stimuli-responsiveness and controlled release ability. The spectrum of applications can be further expanded by its tunable synthesis processes, varied shell thicknesses, and adjustable core sites.

■ EXPERIMENTAL SECTION

Fabrication of a Multichannel and Multijunction Droplet Microfluidic Device. SU-8 (a negative photoresist from MicroChem) molds are used in classic soft lithography to create these specific poly(-dimethylsiloxane) (PDMS) devices.[69,70] The SU-8 mold was initially created on the silicon wafer using UV photolithography in order to build the microfluidic device.[71] Then, after vacuum degassing, the uniform premixed 10:1 combination of Sylgard 184 PDMS (Dow Corning, Midland, MI) and cross-linker was poured into the SU-8 mold and cured. To construct inlets and outlets, PDMS microdevices were excised with a metal scalpel and pierced with 0.75 or 1.0 mm biopsy punches (Harris Uni-Core, Ted Pella, Inc., Redding, CA). Following oxygen plasma activation of both surfaces, PDMS microdevices were then attached to a glass slide and baked at 65 °C for 1 h. To make the channel surface hydrophobic, Aquapel (PGW autoglass LLC.) was used to functionalize the device through hydrophobic treatment.[72]

Synthesis of CdSe Nanocrystals. A 208 cm long microchannel constructed of a 153 cm stainless steel (SS) tube, a 40 cm PTFE tube, and a 15 cm poly(tetrafluoroethylene) (PTFE) tube was used to conduct the synthesis. The size of the interior was 0.75 mm. The SS tubing was utilized as the second part because of its high-temperature stability and good thermal conductivity, and the first and third sections with PTFE tubing were coupled to the collector and the syringe in a flexible manner. A tube furnace was utilized for heating the reaction solution in the SS tubing to the appropriate temperature (150−300 °C), and a syringe pump was employed to regulate the rate of injection. The flow velocity, microchannel diameter, and length all contributed to the residence duration of the reaction solution in the heating zone. This microfluidic device has been described in detail in our past work.[73]

Cadmium oxide (0.54 g, 4 mmol), oleic acid (11 mL, 35 mmol), and 1-octadecene (9 mL, 28 mmol) were heated at 180 °C in a quartz cuvette under nitrogen protection with continuous magneton stirring to give the Cd precursor solution. A pale-yellow mixture is produced at this temperature after an hour. The oil bath was then switched off, and the solution inside the oil was allowed to cool for an additional 30 min to reach a temperature of ∼120 °C. A 20 mL solution of Cd oleate was then made. To make 20 mL of a Se-TOP solution, selenium powder (0.159 g, 2 mmol), TOP (4.5 mL, 12 mmol), and 1-octadecene (14.5 mL, 45 mmol) were combined with magneton stirring under continuously replenished nitrogen in a beaker at room temperature. The Se precursor solution was then swiftly and

https://doi.org/10.1021/acs.langmuir.3c02579
Langmuir XXXX, XXX, XXX−XXX

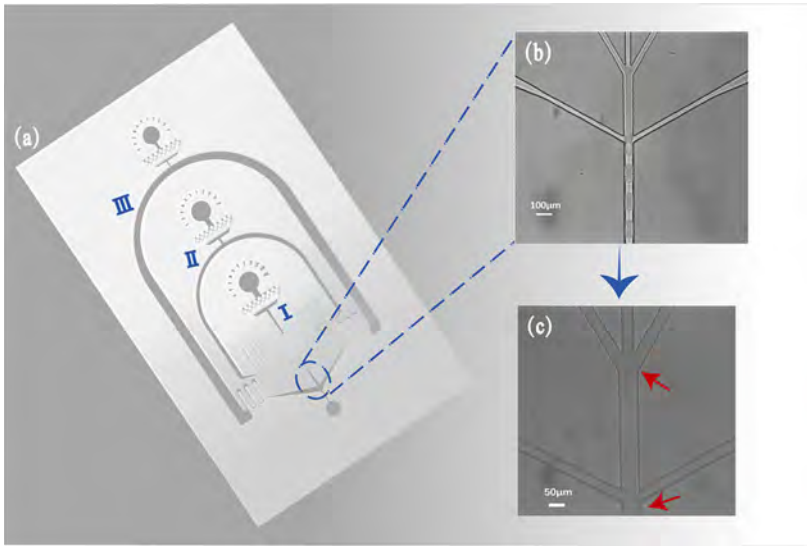

Figure 1. Microstructure of the multichannel and multijunction droplet microfluidic device designed for synthesizing core–shell hydrogel microcapsules (a): optical image of the multijunction droplet microfluidic reactor that is utilized to form core–shell microhydrogels (b); magnified part showing the core flow and the shell flow with a clear boundary (c).

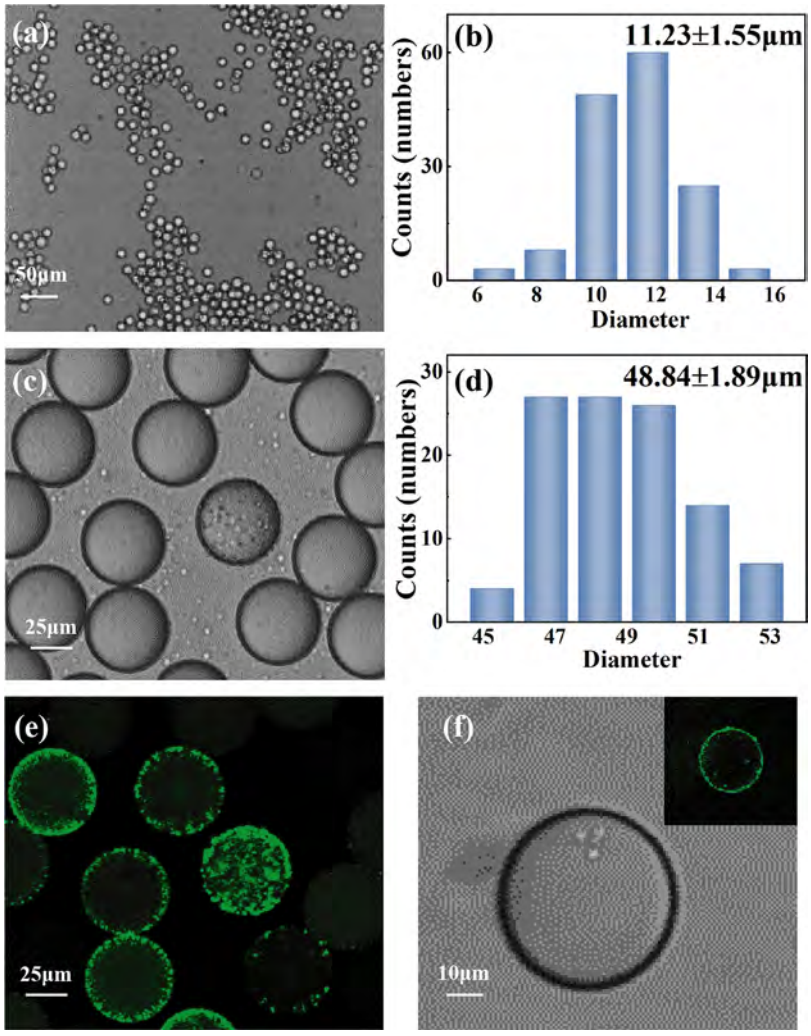

Figure 2. Different diameters of the hydrogel microcapsules were produced by varying the channel size of the microfluidic device. White light optical images (a, c, f), size distribution (b, d), and fluorescent optical images (e, f) of the formed microhydrogel droplets.

https://doi.org/10.1021/acs.langmuir.3c02579
Langmuir XXXX, XXX, XXX−XXX

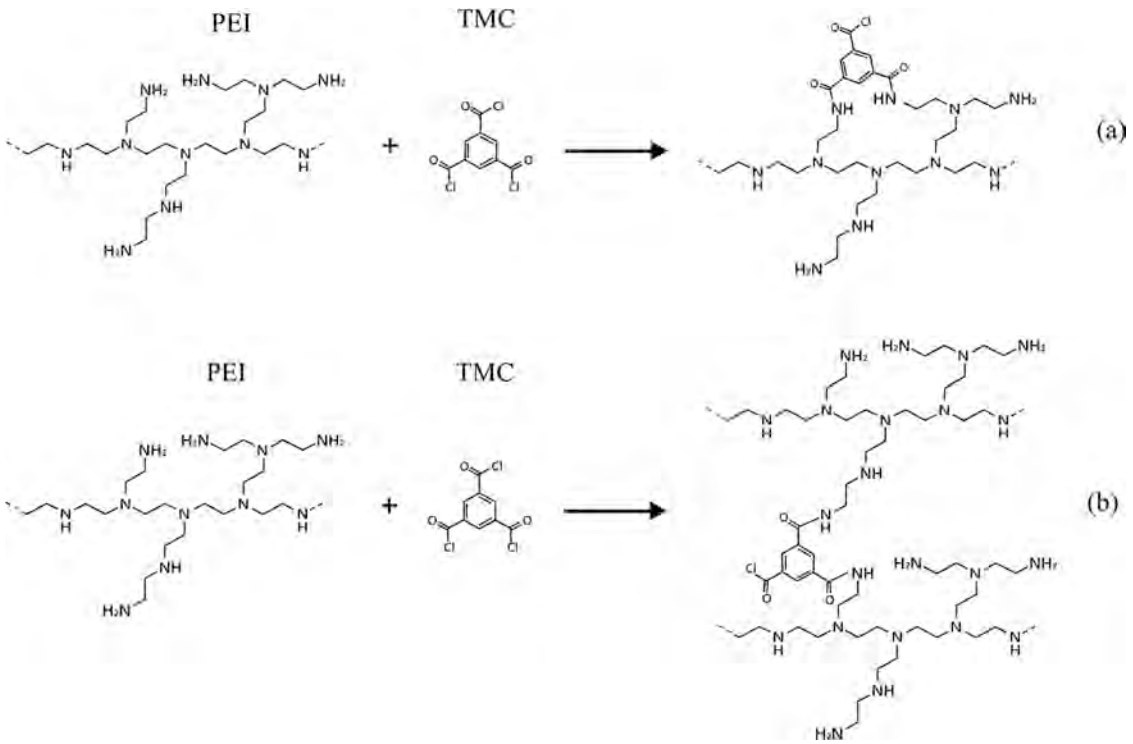

Figure 3. Interfacial polymerization using polyethylenimine (PEI) was employed to form thin and dense membranes between PEI and trimesoyl chloride (TMC): (a) inner-molecule cross-linking; (b) intermolecule cross-linking.

consistently injected into the cadmium oleate solution after it was breathed into a syringe. The preparation of the CdSe precursor solution required 10 min of stirring in nitrogen. A 50 mL syringe that was mounted to the platform of the syringe pump was filled with the CdSe precursor solution. The precursor solution was then injected at the rate of 0.6 mL/min into a microfluidic channel. Initiations of the reaction were performed at 150, 200, 250, and 300 °C. Anhydrous ethanol was used to collect and precipitate the final solution. The centrifugation procedure was then carried out for 10 min at a speed of 13,000 rpm. Decanting was performed with the top supernatant. The NCs that had precipitated were once more distributed in toluene. After a small amount of anhydrous ethanol was added, the CdSe NCs were once more precipitated by centrifugation at a speed of 13,000 rpm for 10 min. The desired NC powder was obtained after the washing procedure twice. After being redispersed into toluene, the product was stored for future use.[73]

Synthesis of Core−Shell Hydrogel Microcapsules with Polyamide Skins as Shells. The core−shell hydrogel microcapsules with PAM shells were synthesized by using the apparatus shown in Figure 1. Channel I is used to inject core materials (5.0 wt % GelMA[74−76] solution); channel II is used to inject shell materials (CdSe encapsulating 10.0 wt % acrylamide solution). Channel III is used to inject oil (PFE) to provide shear force to form drops. Following the collection of these microhydrogel drops in the sample vial, they were exposed to UV light for about 5 min.

Synthesis Conditions of GelMA @ Alginate/PEI Microcapsules with a York-Shell Structure. Synthesis conditions: 4 wt % GelMA aqueous solution in the center flows to form cores at a flow rate of 100−150 μL/min; 1.7 wt % alginate and 2.5 wt % polyethylenimine (PEI) in the middle flow to form shells, at a flow rate of 100−150 μL/min; the outer PFE oil as the drop cutting flows at a flow rate of 800−2000 μL/min; and the droplet collection solution cross-linked by alginic acid salt and PEI was solidified with 0.15 wt % acetic acid (HAc) and 4 mg/mL trimethyl chloride (TMC).

■ RESULTS AND DISCUSSION

Synthesis Device and Optical Imaging of Hydrogel Microcapsules with PAM Shells. Figure 1 depicts the microstructure of multichannel and multijunction droplet microfluidic devices designed for synthesizing core−shell hydrogel microcapsules with polyamide shells. The 5.0 wt % GelMA[74−76] solution was used as the core flow (channel I), the CdSe encapsulating the 10.0 wt % acrylamide solution was utilized as the shell flow (channel II), and PFE was employed as the shear flow (channel III). These flows will meet at the multijunction area as a blue-dotted circle to obtain the core−shell microdroplets.

An optical image of the microfluidic reactor is presented in Figure 1a,b. From Figure 1a, it can be seen that this device can form uniform microdroplets, and Figure 1b is a magnified optical image showing a clear boundary between the core and shell streams.

To produce hydrogel microcapsules that vary in diameter, we designed adaptable microfluidic devices with channels of varying sizes. Specifically, we created devices with 8 and 30 μm channels to synthesize microcapsules that have average diameters of 11.23 μm (Figure 2a,b) and 48.84 μm (Figure 2c,d), respectively. This design allows for the accommodation of drugs or cells of different sizes.

Additionally, using CdSe nanocrystals, we observed the thin-shell structure of the microcapsules. Since CdSe is only added to the shell portion, a confocal fluorescent (PL) microscope was employed to determine if this technique can create core−shell microstructure by comparing the PL intensities of the shell and the core. In Figure 2, optical pictures of cross-linked hydrogel microcapsules are shown. Photographs of the microcapsules in white light and fluorescence of a typical core−shell structured hydrogel microcapsule have been shown in panels c and e, respectively. The PL intensity differs between

https://doi.org/10.1021/acs.langmuir.3c02579
Langmuir XXXX, XXX, XXX−XXX

the core and the shell in at least some of the particles, since following UV light exposure to cross-link the shell acrylamide to PAM, CdSe is prevented from diffusing from the shell into the core, even though some of them may diffuse into the core during sample collection.

As anticipated, a large number of particles do exhibit a difference in intensity between their shells and cores, with bright shell layers and slightly darker cores, as illustrated in Figure 2e,f. This result suggests that this kind of microfluidic device and the use of GelMA solution as the core flow and the CdSe encapsulating 10.0 wt % acrylamide solution as the shell flow allow enough time for the components to maintain their flow before UV exposure. Since our exposure method involves exposure of all of these samples in one vial, the top layers will be exposed intensively and the bottom layers will experience low exposure. As a consequence, not all of the shell acrylamide monomers in these particles can be cross-linked as quickly as the top layers. Thus, a few particles still have uniform PL intensity due to the diffusion of CdSe from the shells to the cores.

Thus, core−shell structured hydrogels with hydrogel microcapsules and PAM shells were successfully synthesized. However, since UV exposure may cause damage to some active substances (e.g., proteins/cells), GelMA @ Alginate/PEI microdroplets were developed using a chemical cross-linking method.

Synthesis Device and Characterization of Core−Shell Structured GelMA @Alginate/PEI Microcapsules with a Core on the Droplet Side. Ca^{2+} cross-linked alginate was also employed as shells to construct a core−shell architecture. It was found that the Ca^{2+} cross-linked alginate was not so tight to prevent CdSe diffusion into the core and the PFE oil solution, leading to the spread of CdSe everywhere in the hydrogels and the oil phase. This means that the pore size in the Ca^{2+} cross-linking alginate is too large, allowing the CdSe to diffuse freely. It was found that the use of Ca^{2+} cross-linked alginate only as shells does not furnish small-size pores. Hence, other methods were employed to fabricate the shell with small pore sizes.

Therefore, interfacial polymerization using polyethylenimine (PEI) was employed to form thin and dense membranes between PEI and trimesoyl chloride (TMC) (see the typical cross-linking reactions: Figure 3(a) inner-molecule cross-linking; Figure 3(b), the intermolecule cross-linking, similar as the polycondensation and cross-linking reaction between TMC and phenylenediamine to form the dense skin layer of the nanofiltration thin film composite membrane.[77,78]) A novel polymer alloy shell was formed by interpenetration between the Ca^{2+} cross-linking alginate and the polyethylenimide, which functioned quite well. The core diameter and the total diameter of droplets can be flexibly controlled.

More importantly, the cross-linking of PEI releases acid, which lowers the pH near the shell layer, and alginate forms acidic gels under acidic conditions, so the decrease in pH causes the shell layer viscosity to increase, thus maintaining the core−shell structure.

After these hydrogel drops are transferred into slightly basic aqueous media (e.g., pH = 8), the chloride ligands will be hydrolyzed into −OH ligands to increase their hydrophilic property, which favors an increase in their biocompatibility.

For the synthesis of GelMA @Alginate/PEI microcapsules, the microfluidic device shown in Figure 4 was prepared based on Figure 1. Channel I is used to inject core materials (e.g., GelMA) for drug encapsulation; channel II is used to inject shell materials (e.g., alginate or monomer for polymeric gels) for drug or cell encapsulation. Channel III is used to inject oil (e.g., PFE) to provide a shear force to form drops. Channel IV will provide some reagents in oil (e.g., acetic acid to solidify the shell materials). These flows will meet at the multijunction area shown as the red-dotted circle to obtain the core−shell drops.

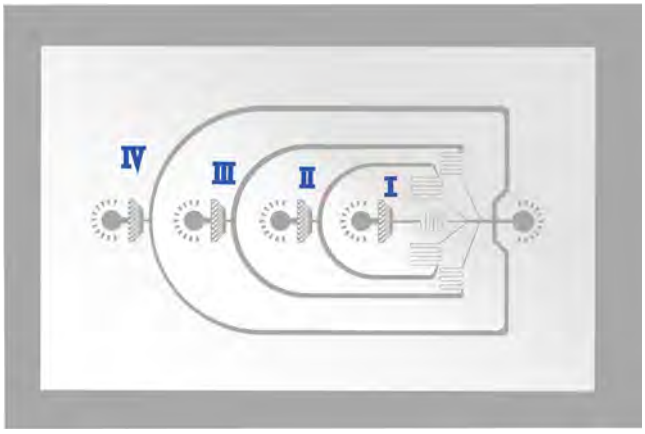

Figure 4. Microstructure of the multichannel and multijunction droplet microfluidic device designed for the synthesis of core−shell hydrogel microparticles for the synthesis of GelMA @Alginate/PEI microcapsules.

The typical confocal fluorescent images and the corresponding bright-field image of these core−shell hydrogel droplets clearly show their core (fluorescent color)−shell structures (Figure 5). The core is biased, and many cores are in contact with the shell due to the same channel depth and geometry between the core flow and the shell flow. Some drops collapse to form month shapes, possibly due to the thin, dense outer membrane formed by polyimide.

In addition to synthesizing microcapsules of varied diameters using differing channel sizes, we adjusted the flow rates of the two phases to control both the core and total diameters.

When the PFE oil flow rate was 800 μL/min, the average total diameter of the microcapsules was 52.28 μm and the core diameter was 18.80 μm (Figure 5a−c); when the PFE oil flow rate was 2000 μL/min, the average total diameter of the microcapsules was 42.01 μm and the core diameter was 21.50 μm (Figure 5e−g). This demonstrates that the diameter of microcapsules becomes smaller with a faster flow rate of PFE oil.

Additionally, the core was labeled with FITC to facilitate the core position observation and enhance visualization of the core−shell structure. Figure 5d,h displays typical optical images and corresponding confocal fluorescence images of the hydrogel microcapsules with a core−shell.

Synthesis and Characterization of Core−Shell Structured GelMA @Alginate/PEI Microcapsules with the Core Located in the Center of the Droplet. The PDMS microfluidic device shape was tuned so that the oil-cutting flow in channel III arrives in a horizontal direction to obtain droplets with cores positioned in the centers of the droplets (Figure 6). To produce the channel junction with the core channel precisely in the middle of the shell channel, a multistep exposure and mask alignment approach was adopted.

As is evident in their bright-field image in Figure 7a, the encapsulation can result in core−shell droplet hydrogels, with

https://doi.org/10.1021/acs.langmuir.3c02579
Langmuir XXXX, XXX, XXX−XXX

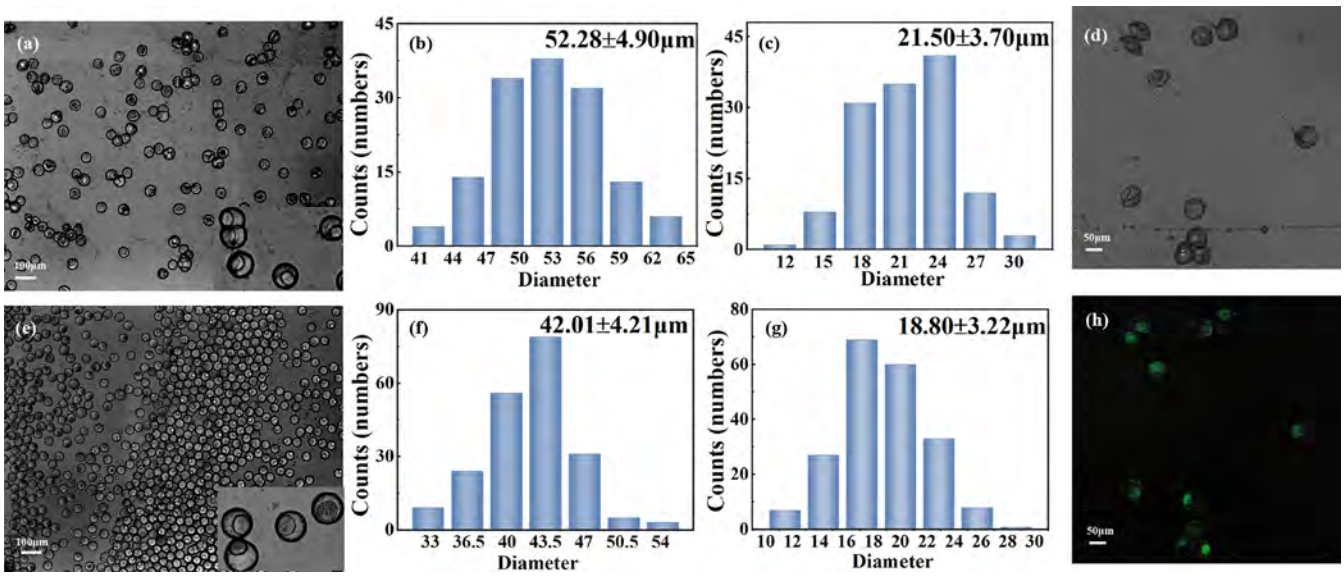

Figure 5. Bright-field optical images and size distribution of core−shell GelMA @ Alginate/PEI microcapsules. (a−c) Microcapsules with an average core diameter of 21.50 μm and an average total diameter of 52.28 μm at a PFE oil flow rate of 800 μL/min. (e−g) Microcapsules with an average core diameter of 18.80 μm and an average total diameter of 42.01 μm at a PFE oil flow rate of 2000 μL/min. (d) Typical bright-field image and (h) the corresponding confocal fluorescent images of these core−shell hydrogel microcapsules.

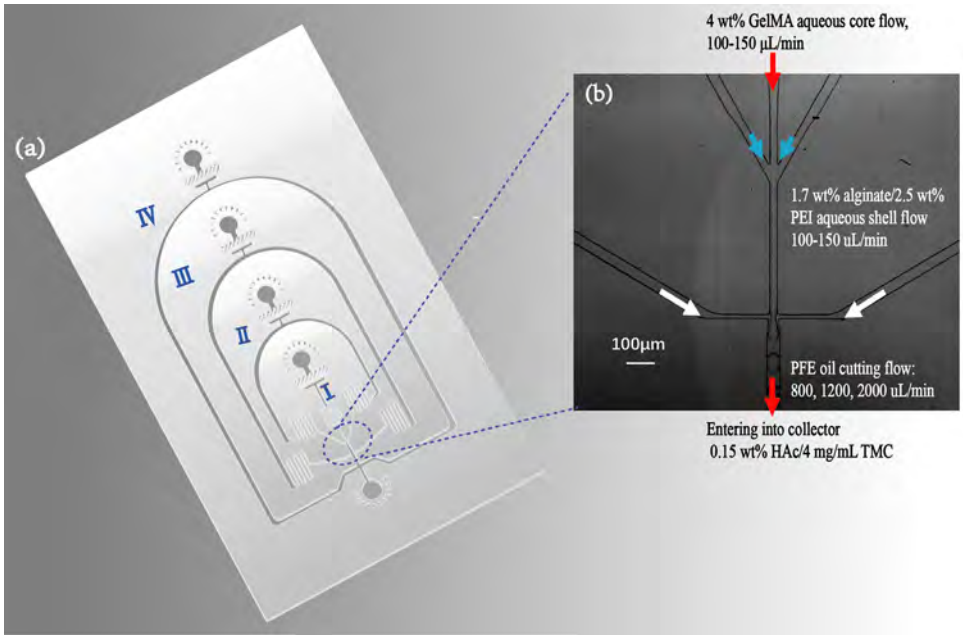

Figure 6. Geometry and channel size optimized multijunction microfluidic reactor for synthesis of core−shell drops with cores in the center of drops; (a) local amplified bright-field images of microfluidic devices and conditions for synthesizing microcapsules with a core−shell structure.

the majority of their cores located at the center of the entire droplet. The core−shell structures are visible in the confocal fluorescence image (Figure 7b) of one representative area of these droplets on the glass slip and present the majority of the cores in the center of the drops. Additionally, the magnified image in Figure 7b's upper right corner demonstrates a brighter fluorescence on the outer surface of the core, which is caused by interfacial tension.

When Rhodamine B is added to PEI after external cross-linking, the thin shell can be seen under confocal imaging, indicating that PEI has been adequately cross-linked (Figure 7c,d). In this case, the core−shell structure becomes more stable, the alginate viscosity increases, and the pH near the shell layer lowers. The microcapsule had an average total diameter of 32.85 μm and a core diameter of 14.30 μm (Figure 7e,f).

Stimuli-Responsiveness and Controlled Release of Hydrogel Microcapsules. We also investigated the thermal effects on the nanomedicine encapsulating hydrogel particles, which is important in the discovery of the hyperthermal controlled release of drugs since we have found that the GelMA can be a gel at room temperature and a solution at elevated temperatures.

To study the temperature-responsiveness of hydrogel microcapsules, metal-based nanomedicines developed by our group were encapsulated in hydrogel microcapsules.[79,80] Figure

https://doi.org/10.1021/acs.langmuir.3c02579
Langmuir XXXX, XXX, XXX−XXX

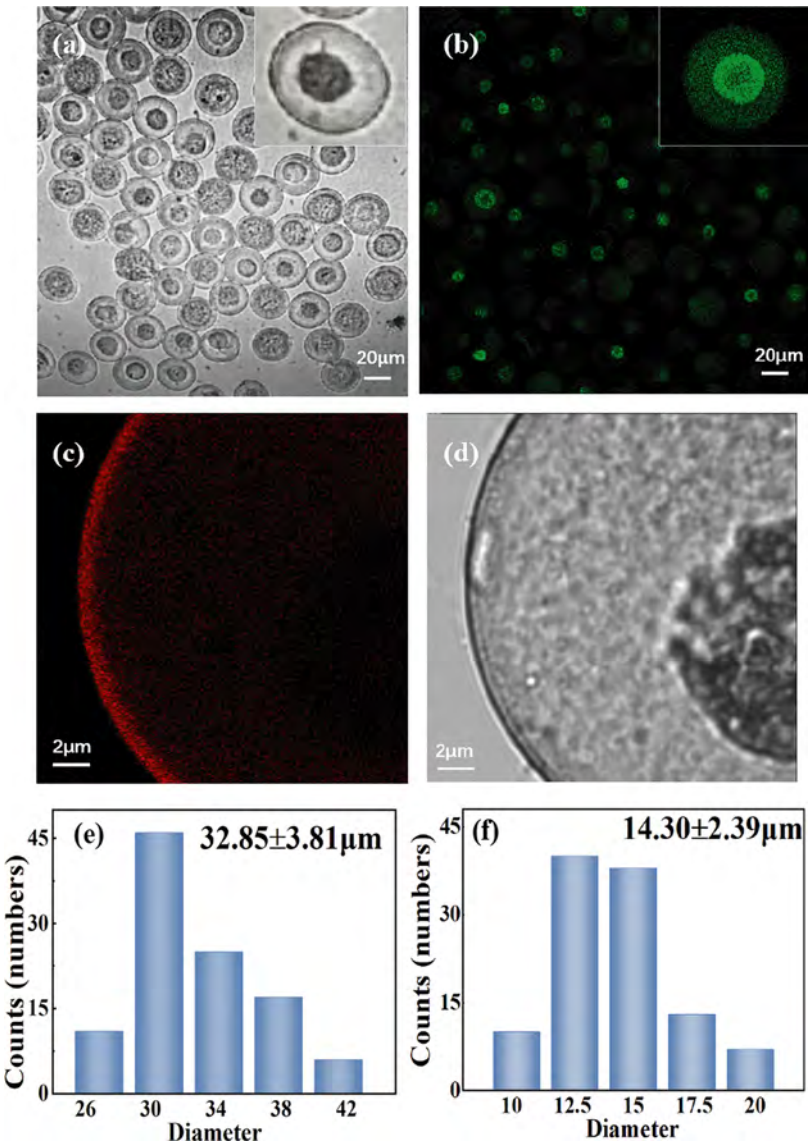

Figure 7. (a) Bright-field image showing most cores at the center of drops; (b) confocal fluorescent image. (c, d) By adding Rhodamine B to PEI, the thin shell can be observed under the confocal microscope after external cross-linking. The diameter distribution of the total (e) and the core (f).

8a,8b shows the optical images of metal-based nanomedicines encapsulated into hydrogel microcapsules with a PAM skin as the shell synthesized using a droplet microfluidic device with the final channel size of 8 μm (a, concentrated area; b, diluted area). Figure 8d,8e displays the optical images of metal-based nanomedicines encapsulated into the hydrogel microcapsules after being annealed at 37 °C for 6 h. Clearly, numerous small particles appear in these samples, and their size distribution becomes broader, indicating that annealing at a high temperature can break the stability of these microgels, which is advantageous for thermally controlled drug release. These microcapsules show great potential for the creation of temperature-responsive drug delivery systems for use on living organisms and skin surfaces. Their ability to provide controlled release of drugs makes them valuable tools in pharmaceutical development.

The controlled release performance of GelMA @Alginate/PEI microcapsules was observed under dark-field microscopy conveniently thanks to the localized surface plasmon resonance (LSPR) scattering of this metal-based nanomedicine.[79,80] After the core−shell droplets with shells made of nanomedicines encapsulated into the cross-linked alginate-PEI, the droplets are transferred into the phosphate-buffered saline (PBS) buffer and the gradually releasing of nanomedicines from shells into cores is characterized under a dark-field microscope.

On day 1, Figure 9 illustrates the absence of LSPR colorful scattering in the droplet cores. However, on day 3, distinct colorful scattering is observable in the droplet cores, and by day 5, the entire core−shell droplets display distinct colorful scattering with no distinguishable difference in LSPR scattering between cores and shells. This result indicates that the nanomedicines in the shells can be gradually and slowly diffused into the GelMA cores in 3−5 days, which gives us enough time to observe the drug−cell interaction by the controlled release of nanomedicines into the microenvironment of cells. The core−shell structured microcapsules can be utilized to analyze cell/drug interactions by regulating the release of nanomedicines.

https://doi.org/10.1021/acs.langmuir.3c02579
Langmuir XXXX, XXX, XXX−XXX

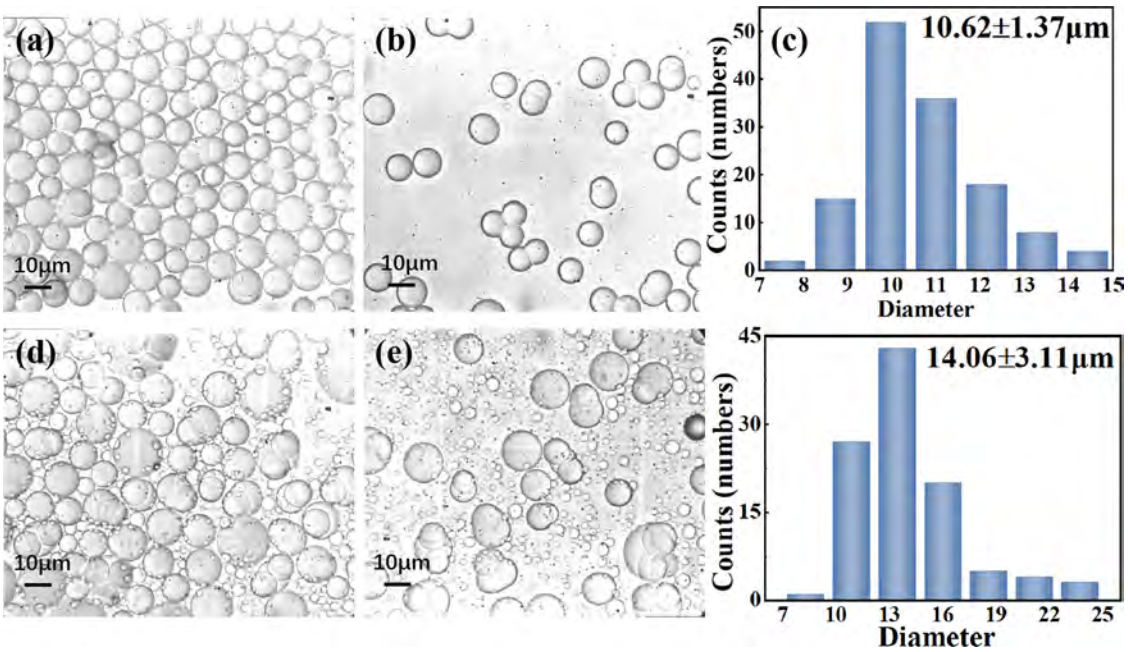

Figure 8. Optical image of metal-based nanomedicines encapsulated into hydrogel microcapsules with a PAM skin as the shell (a, d: concentrated area; b, e: diluted area). Morphology and diameter distribution of hydrogel microcapsules at room temperature (a–c) and after heating at 37 °C for 6 h (d–f).

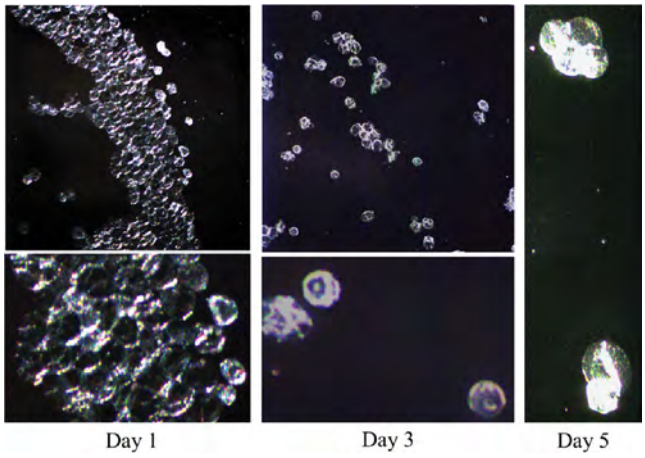

Figure 9. Controlled release of nanomedicines in the shells (made of alginate and PEI cross-linking by TMC) of hydrogel droplets into the core (GelMA) of hydrogel droplets observed under a dark-field microscope based on LSPR scattering of metal-based nanomedicines.

■ CONCLUSIONS

In summary, we designed and prepared several multichannel and multifunctional droplet microfluidic devices based on soft lithography. Different forms of hydrogel microcapsules with core–shell structures were prepared using characteristic devices and by employing different cross-linking techniques. Among them, hydrogel microcapsules with GelMA as the core and PAM skin as the thin shell were synthesized using a UV-based cross-linking process. This cost-efficient cross-linking process allows for the convenient and efficient synthesis of core–shell structured microcapsules suitable for encapsulation and transport of UV-resistant substances.

Moreover, for the transport of UV-sensitive bioactives, we used an interfacial polymerization process for cross-linking to construct core–shell structured hydrogel microcapsules. This microgel has GelMA as the core and Ca^{2+} cross-linked alginate with PEI as the shell, and the core diameter and total droplet diameter are flexibly controlled by sculpting. The microcapsule is thus well suited for the transport of two different substances.

Based on the above template, the geometry of the PDMS microfluidic device was optimized and prepared using multistep exposure and mask alignment techniques to have the core of the core–shell hydrogel droplet located in the center. A channel junction with the core channel exactly at the center of the shell channel was prepared, and the core of the synthesized core–shell hydrogel droplet was located in the center. These microcapsules are suitable for the transport of multiple substances with a reduced risk of leakage.

Additionally, precise control of the core and total diameters of these droplets is achievable through the variation of the channel size and the flow rates of the two phases (i.e., GelMA and PFE). In particular, the size of the microchannels has a significant effect on the diameter of the droplets, with channels of about 30 μm diameter suitable for encapsulation of cells or drugs and smaller channels of around 8 μm diameter appropriate for drug encapsulation. On the other hand, the core diameter and total diameter can be adjusted in small increments using the cutting PFE oil flow. This adaptable diameter control permits precise encapsulation of various contents.

More importantly, these hydrogel microcapsules exhibit stimuli-responsiveness and controlled release ability, providing an advantage in the kinetic regulation of multi-drug or cell delivery. The microcapsules can be applied in a wide range of fields and have potential for high-throughput drug screening, as well as delivering multiple cells or drugs and the visible investigation of the drug–cell interaction.

https://doi.org/10.1021/acs.langmuir.3c02579
Langmuir XXXX, XXX, XXX–XXX

AUTHOR INFORMATION

Corresponding Author

Yujun Song − *Center for Modern Physics Technology, School of Mathematics and Physics, University of Science and Technology Beijing, Beijing 100083, China; Physics Department, School of Engineering and Applied Science, Harvard University, Cambridge, Massachusetts 02138, United States; Zhengzhou Tianzhao Biomedical Technology Company Ltd., Zhengzhou 451450, China; Key Laboratory of Pulsed Power Translational Medicine of Zhejiang Province, Hangzhou 310003, China;* orcid.org/0000-0003-2474-084X; Email: songyj@ustb.edu.cn

Authors

Qiong Wu − *Center for Modern Physics Technology, School of Mathematics and Physics, University of Science and Technology Beijing, Beijing 100083, China*

Xing Huang − *Physics Department, School of Engineering and Applied Science, Harvard University, Cambridge, Massachusetts 02138, United States; Department of Mechanical Engineering and Zhejiang Provincial Engineering Center of Integrated Manufacturing Technology and Intelligent Equipment, Hangzhou City University, Hangzhou 310015, China*

Ran Liu − *Center for Modern Physics Technology, School of Mathematics and Physics, University of Science and Technology Beijing, Beijing 100083, China; Zhengzhou Tianzhao Biomedical Technology Company Ltd., Zhengzhou 451450, China; Key Laboratory of Pulsed Power Translational Medicine of Zhejiang Province, Hangzhou 310003, China*

Xinzhu Yang − *Center for Modern Physics Technology, School of Mathematics and Physics, University of Science and Technology Beijing, Beijing 100083, China; Zhengzhou Tianzhao Biomedical Technology Company Ltd., Zhengzhou 451450, China; Key Laboratory of Pulsed Power Translational Medicine of Zhejiang Province, Hangzhou 310003, China*

Gao Xiao − *Physics Department, School of Engineering and Applied Science, Harvard University, Cambridge, Massachusetts 02138, United States; Department of Environmental Science and Engineering, College of Environment and Safety Engineering, Fuzhou University, Fuzhou 350108, China*

Nan Jiang − *Physics Department, School of Engineering and Applied Science, Harvard University, Cambridge, Massachusetts 02138, United States; West China School of Basic Medical Sciences & Forensic Medicine, Sichuan University, Chengdu 610041, China; JinFeng Laboratory, Chongqing 401329, China;* orcid.org/0000-0001-8394-3247

David A. Weitz − *Physics Department, School of Engineering and Applied Science, Harvard University, Cambridge, Massachusetts 02138, United States;* orcid.org/0000-0001-6678-5208

Complete contact information is available at: https://pubs.acs.org/10.1021/acs.langmuir.3c02579

Author Contributions

¶Q.W. and X.H. contributed equally to this work.

Notes

The authors declare no competing financial interest.

ACKNOWLEDGMENTS

This study was financially supported by the National Natural Science Foundation of China (No. 51971029), the BRICS STI Framework Programmed by NSFC (No. 51861145309), the National S&T Major Project of China (No. 2018ZX10301201), the development of a highly sensitive magneto-optical biomolecular sensor experimental prototype (contract no. in USTB: 2019-0649), and the probability analysis of nanoknife coupling nanomedicine for combined anticancer therapy from Zhejiang Key Laboratory for Pulsed Power Translational Medicine through Hangzhou Ruidi Biotechnology Co., Ltd., and the 1125 Zhihui Zhengzhou Talent Project of Henan province (fund no. in USTB: 39080070) from Zhengzhou Tianzhao Biomedical Technology Co. Ltd.

ABBREVIATIONS

GelMA, gelatin methacryloyl; PEI, polyethylenimine; PDMS, poly(-dimethylsiloxane); RGD, Arg-Gly-Asp; AM, acrylamide; SA, sodium alginate; SS, stainless steel; PTFE, poly-(tetrafluoroethylene); PEI, polyethylenimine; HAc, acetic acid; TMC, trimethyl chloride; PL, confocal fluorescent; PEI, polyethylenimine; LSPR, localized surface plasmon resonance

REFERENCES

(1) Hoare, T. R.; Kohane, D. S. Hydrogels in Drug Delivery: Progress and Challenges. *Polymer* **2008**, *49*, 1993−2007.

(2) Kamachi, Y.; Bastakoti, B. P.; Alshehri, S. M.; Miyamoto, N.; Nakato, T.; Yamauchi, Y. Thermo-Responsive Hydrogels Containing Mesoporous Silica toward Controlled and Sustainable Releases. *Mater. Lett.* **2016**, *168*, 176−179.

(3) Balakrishnan, B.; Banerjee, R. Biopolymer-Based Hydrogels for Cartilage Tissue Engineering. *Chem. Rev.* **2011**, *111*, 4453−4474.

(4) Kabiri, K.; Faraji-Dana, S.; Zohuriaan-Mehr, M. J. Novel Sulfobetaine-Sulfonic Acid-Contained Superswelling Hydrogels. *Polym. Adv. Technol.* **2005**, *16* (9), 659−666.

(5) Liang, X.; Deng, Y.; Pei, X.; Zhai, K.; Xu, K.; Tan, Y.; Gong, X.; Wang, P. Tough, Rapid-Recovery Composite Hydrogels Fabricated via Synergistic Core−Shell Microgel Covalent Bonding and Fe^{3+} Coordination Cross-Linking. *Soft Matter* **2017**, *13* (14), 2654−2662.

(6) Nemoto, H.; Shimba, D.; Kanai, T. Preparation of Monodisperse Silica-Polyacrylamide Hybrid Particles with Snowman or Core-Shell Morphologies Using a Microfluidic Device. *J. Asian Ceram Soc.* **2022**, *10* (2), 378−385.

(7) Brannon-Peppas, L.; Peppas, N. A. Dynamic and Equilibrium Swelling Behaviour of PH-Sensitive Hydrogels Containing 2-Hydroxyethyl Methacrylate. *Biomaterials* **1990**, *11* (9), 635−644.

(8) Gemeinhart, R. A.; Chen, J.; Park, H.; Park, K. PH-Sensitivity of Fast Responsive Superporous Hydrogels. *J. Biomater. Sci., Polym. Ed.* **2000**, *11* (12), 1371−1380.

(9) Hirose, Y.; Amiya, T.; Hirokawa, Y.; Tanaka, T. Phase Transition of Submicron Gel Beads. *Macromolecules* **1987**, *20* (6), 1342−1344.

(10) Tanaka, T.; Sato, E.; Hirokawa, Y.; Hirotsu, S.; Peetermans, J. Critical Kinetics of Volume Phase Transition of Gels. *Phys. Rev. Lett.* **1985**, *55* (22), 2455−2458.

(11) Brownlee, M.; Cerami, A. A Glucose-Controlled Insulin-Delivery System: Semisynthetic Insulin Bound to Lectin. *Science* **1979**, *206* (4423), 1190−1191.

(12) Park, T. G.; Hoffman, A. S. Sodium Chloride-Induced Phase Transition in Nonionic Poly(N-Isopropylacrylamide) Gel. *Macromolecules* **1993**, *26* (19), 5045−5048.

(13) Bromberg, L.; Temchenko, M.; Alakhov, V.; Hatton, T. A. Kinetics of Swelling of Polyether-Modified Poly(Acrylic Acid) Microgels with Permanent and Degradable Cross-Links. *Langmuir* **2005**, *21* (4), 1590−1598.

(14) Ghandehari, H.; Kopecková, P.; Kopecek, J. In Vitro Degradation of PH-Sensitive Hydrogels Containing Aromatic Azo Bonds. *Biomaterials* **1997**, *18* (12), 861−872.
(15) Chen, J.; Blevins, W. E.; Park, H.; Park, K. Gastric Retention Properties of Superporous Hydrogel Composites. *J. Controlled Release* **2000**, *64* (1−3), 39−51.
(16) Nguyen, K. T.; West, J. L. Photopolymerizable Hydrogels for Tissue Engineering Applications. *Biomaterials* **2002**, *23* (22), 4307−4314.
(17) Bashir, R.; Hilt, J. Z.; Elibol, O.; Gupta, A.; Peppas, N. A. Micromechanical Cantilever as an Ultrasensitive PH Microsensor. *Appl. Phys. Lett.* **2002**, *81* (16), 3091−3093.
(18) El-Hag Ali, A.; Shawky, H. A.; Rehim, H. A. A. E.; Hegazy, E. A. Synthesis and Characterization of PVP/AAc Copolymer Hydrogel and Its Applications in the Removal of Heavy Metals from Aqueous Solution. *Eur. Polym. J.* **2003**, *39* (12), 2337−2344.
(19) Atta, A. M.; Ismail, H. S.; Mohamed, H. M.; Mohamed, Z. M. Acrylonitrile/Acrylamidoxime/2-acrylamido-2- Methylpropane Sulfonic Acid-based Hydrogels: Synthesis, Characterization and Their Application in the Removal of Heavy Metals. *J. Appl. Polym. Sci.* **2011**, *122* (2), 999−1011.
(20) Annaka, M.; Matsuura, T.; Kasai, M.; Nakahira, T.; Hara, Y.; Okano, T. Preparation of Comb-Type N-Isopropylacrylamide Hydrogel Beads and Their Application for Size-Selective Separation Media. *Biomacromolecules* **2003**, *4* (2), 395−403.
(21) Tumarkin, E.; Kumacheva, E. Microfluidic Generation of Microgels from Synthetic and Natural Polymers. *Chem. Soc. Rev.* **2009**, *38* (8), 2161−2168.
(22) Malmsten, M.; Bysell, H.; Hansson, P. Biomacromolecules in Microgels—Opportunities and Challenges for Drug Delivery. *Curr. Opin. Colloid Interface Sci.* **2010**, *15* (6), 435−444.
(23) Yang, B.; Lu, Y.; Ren, T.; Luo, G. One-Step Synthesis of PH-Sensitive Poly(Acrylamide-Co-Sodium Acrylate) Beads with Core−Shell Structure. *React. Funct. Polym.* **2013**, *73* (1), 122−131.
(24) Madene, A.; Jacquot, M.; Scher, J.; Desobry, S. Flavour Encapsulation and Controlled Release − a Review. *Int. J. Food Sci. Technol.* **2006**, *41*, 1−21, DOI: 10.1111/j.1365-2621.2005.00980.x.
(25) Mcclements, D. J.; Decker, E. A.; Weiss, J. Emulsion-Based Delivery Systems for Lipophilic Bioactive Components. *J. Food Sci.* **2010**, *72* (8), R109−R124, DOI: 10.1111/j.1750-3841.2007.00507.x.
(26) Pea, B.; Panisello, C.; Aresté, G.; Garcia-Valls, R.; Gumí, T. Preparation and Characterization of Polysulfone Microcapsules for Perfume Release. *Chem. Eng. J.* **2011**, *179* (1), 394−403, DOI: 10.1016/j.cej.2011.10.090.
(27) Jacquemond, M.; Jeckelmann, N.; Ouali, L.; Haefliger, O. P. Perfume-Containing Polyurea Microcapsules with Undetectable Levels of Free Isocyanates. *J. Appl. Polym. Sci.* **2009**, *114* (5), 3074−3080.
(28) Zhao, C. X. Multiphase Flow Microfluidics for the Production of Single or Multiple Emulsions for Drug Delivery. *Adv. Drug Delivery Rev.* **2013**, *65* (11−12), 1420−1446.
(29) Comiskey, B.; Albert, J. D.; Yoshizawa, H.; Jacobson, J. An Electrophoretic Ink for All-Printed Reflective Electronic Displays. *Nature* **1998**, *394*, 253−255.
(30) Usami, T.; Igarashi, A. The Development of Direct Thermal Full Color Recording Material. *J. Photogr Soc. Jpn.* **1996**, *58* (4), 347−357.
(31) Zhang, C.; Gao, W.; Zhao, Y.; Chen, Y. Microfluidic Generation of Self-Contained Multicomponent Microcapsules for Self-Healing Materials. *Appl. Phys. Lett.* **2018**, *113* (20), No. 203702.
(32) Yang, J.; Keller, M. W.; Moore, J. S.; White, S. R.; Sottos, N. R. Microencapsulation of Isocyanates for Self-Healing Polymers. *Macromolecules* **2008**, *41* (24), 9650−9655.
(33) Xu, S.; Nisisako, T. Polymer Capsules with Tunable Shell Thickness Synthesized via Janus-to-Core Shell Transition of Biphasic Droplets Produced in a Microfluidic Flow-Focusing Device. *Sci. Rep.* **2020**, *10* (1), No. 4549.
(34) Mytnyk, S.; Ziemecka, I.; Olive, A. G. L.; van der Meer, J. W. M.; Totlani, K. A.; Oldenhof, S.; Kreutzer, M. T.; van Steijn, V.; van Esch, J. H. Microcapsules with a Permeable Hydrogel Shell and an Aqueous Core Continuously Produced in a 3D Microdevice by All-Aqueous Microfluidics. *Rsc Adv.* **2017**, *7*, 11331−11337.
(35) Wei, Y.; Soh, S.; Apodaca, M. M.; Kim, J.; Grzybowski, B. A. Sequential Reactions Directed by Core/Shell Catalytic Reactors. *Small* **2010**, *6* (7), 857−863.
(36) Galogahi, F. M.; Zhu, Y.; An, H.; Nguyen, N. T. Core-Shell Microparticles: Generation Approaches and Applications. *J. Sci.: Adv. Mater. Devices* **2020**, *5* (4), 417−435.
(37) Chong, D.; Liu, X.; Ma, H.; Huang, G.; Han, Y. L.; Cui, X.; Yan, J.; Xu, F. Advances in Fabricating Double-Emulsion Droplets and Their Biomedical Applications. *Microfluid. Nanofluid.* **2015**, *19* (5), 1071−1090.
(38) Liu, H.; Zhang, Y. Droplet Formation in a T-Shaped Microfluidic Junction. *J. Appl. Phys.* **2009**, *106* (3), No. 034906.
(39) Nabavi, S. A.; Vladisavljević, G. T.; Manović, V. Mechanisms and Control of Single-Step Microfluidic Generation of Multi-Core Double Emulsion Droplets. *Chem. Eng. J.* **2017**, *322*, 140−148.
(40) Nisisako, T.; Okushima, S.; Torii, T. Controlled Formulation of Monodisperse Double Emulsions in a Multiple-Phase Microfluidic System. *Soft Matter* **2005**, *1* (1), 23−27.
(41) Utada, A. S.; Lorenceau, E.; Link, D. R.; Kaplan, P. D.; Stone, H. A.; Weitz, D. A. Monodisperse Double Emulsions Generated from a Microcapillary Device. *Science* **2005**, *308* (5721), 537−541.
(42) Galogahi, F. M.; Zhu, Y.; An, H.; Nguyen, N. T. Formation of Core−Shell Droplets for the Encapsulation of Liquid Contents. *Microfluid. Nanofluid.* **2021**, *25* (10), No. 82, DOI: 10.1007/s10404-021-02483-2.
(43) Guerzoni, L. P. B.; Bohl, J.; Jans, A.; et al. Microfluidic fabrication of polyethylene glycol microgel capsules with tailored properties for the delivery of biomolecules. *Biomater. Sci.* **2017**, *5* (8), 1549−1557.
(44) Nguyen, N. T.; Schubert, S.; Richter, S.; Dötzel, W. Hybrid-Assembled Micro Dosing System Using Silicon-Based Micropump/Valve and Mass Flow Sensor. *Sens. Actuators, A* **1998**, *69* (1), 85−91.
(45) Yap, Y. F.; Tan, S. H.; Nguyen, N. T.; Murshed, S. M. S.; Wong, T. N.; Yobas, L. Thermally Mediated Control of Liquid Microdroplets at a Bifurcation. *J. Phys. D: Appl. Phys.* **2009**, *42* (6), No. 065503.
(46) Hennequin, Y.; Pannacci, N.; de Torres, C. P.; Tetradis-Meris, G.; Chapuliot, S.; Bouchaud, E.; Tabeling, P. Synthesizing Microcapsules with Controlled Geometrical and Mechanical Properties with Microfluidic Double Emulsion Technology. *Langmuir* **2009**, *25* (14), 7857−7861.
(47) Peng, S.; Zhang, M.; Niu, X.; Wen, W.; Sheng, P.; Liu, Z.; Shi, J. Magnetically Responsive Elastic Microspheres. *Appl. Phys. Lett.* **2008**, *92*, No. 012108.
(48) Choi, S. W.; Zhang, Y.; Xia, Y. Fabrication of Microbeads with a Controllable Hollow Interior and Porous Wall Using a Capillary Fluidic Device. *Adv. Funct. Mater.* **2009**, *19* (18), 2943−2949.
(49) Windbergs, M.; Zhao, Y.; Heyman, J.; Weitz, D. A. Biodegradable Core-Shell Carriers for Simultaneous Encapsulation of Synergistic Actives. *J. Am. Chem. Soc.* **2013**, *135* (21), 7933−7937.
(50) Tan, W. H.; Takeuchi, S. Monodisperse Alginate Hydrogel Microbeads for Cell Encapsulation. *Adv. Mater.* **2007**, *19* (18), 2696−2701.
(51) Okushima, S.; Nisisako, T.; Torii, T.; Higuchi, T. Controlled Production of Monodisperse Double Emulsions by Two-Step Droplet Breakup in Microfluidic Devices. *Langmuir* **2004**, *20* (23), 9905−9908.
(52) Seo, M.; Paquet, C.; Nie, Z.; Xu, S.; Kumacheva, E. Microfluidic Consecutive Flow-Focusing Droplet Generators. *Soft Matter* **2007**, *3* (8), 986−992.
(53) Chen, C. H.; Abate, A. R.; Lee, D.; Terentjev, E. M.; Weitz, D. A. Microfluidic Assembly of Magnetic Hydrogel Particles with Uniformly Anisotropic Structure. *Adv. Mater.* **2009**, *21* (31), 3201−3204.
(54) Perro, A.; Nicolet, C.; Angly, J.; Lecommandoux, S.; Le Meins, J. F.; Colin, A. Mastering a Double Emulsion in a Simple Co-Flow

Microfluidic to Generate Complex Polymersomes. *Langmuir* **2011**, *27* (14), 9034−9042.
(55) Chu, L. Y.; Utada, A. S.; Shah, R. K.; Kim, J. W.; Weitz, D. A. Controllable Monodisperse Multiple Emulsions. *Angew. Chem., Int. Ed.* **2007**, *46* (47), 8970−8974.
(56) Hafezi, M.; Khorasani, S. N.; Khalili, S.; Neisiany, R. E. Self-Healing Interpenetrating Network Hydrogel Based on GelMA/Alginate/Nano-Clay. *Int. J. Biol. Macromol.* **2023**, *242* (Pt 2), No. 124962.
(57) Rajabi, N.; Rezaei, A.; Kharaziha, M.; Bakhsheshi-Rad, H. R.; Luo, H.; RamaKrishna, S.; Berto, F. Recent Advances on Bioprinted Gelatin Methacrylate-Based Hydrogels for Tissue Repair. *Tissue Eng., Part A* **2021**, *27* (11−12), 679−702.
(58) Bupphathong, S.; Quiroz, C.; Huang, W.; Chung, P. F.; Tao, H. Y.; Lin, C. H. Gelatin Methacrylate Hydrogel for Tissue Engineering Applications—A Review on Material Modifications. *Pharmaceuticals* **2022**, *15* (2), No. 171, DOI: 10.3390/ph15020171.
(59) Pepelanova, I.; Kruppa, K.; Scheper, T.; Lavrentieva, A. Gelatin-Methacryloyl (GelMA) Hydrogels WithDefined Degree of Functionalization as a Versatile Toolkit for 3D Cell Culture and Extrusion Bioprinting. *Bioengineering* **2018**, *5* (3), No. 55, DOI: 10.3390/bioengineering5030055.
(60) Elkhoury, K.; Koak, P.; Kang, A.; Arab-Tehrany, E.; Ellis Ward, J.; Shin, S. R. Engineering Smart Targeting Nanovesicles and Their Combination with Hydrogels for Controlled Drug Delivery. *Pharmaceutics* **2020**, *12* (9), No. 849, DOI: 10.3390/pharmaceutics12090849.
(61) Kadri, R.; Elkhoury, K.; Ben Messaoud, G.; Kahn, C.; Tamayol, A.; Mano, J. F.; Arab-Tehrany, E.; Sánchez-González, L. Physicochemical Interactions in Nanofunctionalized Alginate/GelMA IPN Hydrogels. *Nanomaterials* **2021**, *11* (9), No. 2256, DOI: 10.3390/nano11092256.
(62) Gustavsson, P. E.; Larsson, P. O. Superporous Agarose, a New Material for Chromatography. *J. Chromatogr. A* **1996**, *734* (2), 231−240.
(63) Zhao, K.; Chen, T.; Lin, B.; Cui, W.; Kan, B.; Yang, N.; Zhou, X.; Zhang, X.; Wei, J. Adsorption and Recognition of Protein Molecular Imprinted Calcium Alginate/Polyacrylamide Hydrogel Film with Good Regeneration Performance and High Toughness. *React. Funct. Polym.* **2015**, *87*, 7−14.
(64) Gümüşderelioğlu, M.; Erce, D.; Demirtaş, T. T. Superporous Polyacrylate/Chitosan IPN Hydrogels for Protein Delivery. *J. Mater. Sci.: Mater. Med.* **2011**, *22* (11), 2467−2475.
(65) Guo, S.; Yao, T.; Wang, C.; Zeng, C.; Zhang, L. Preparation of Monodispersed Porous Polyacrylamide Microspheres via Phase Separation in Microchannels. *React. Funct. Polym.* **2015**, *91−92*, 77−84.
(66) Slater, M.; Snauko, M.; Svec, F.; Fréchet, J. M. J. Click Chemistry" in the Preparation of Porous Polymer-Based Particulate Stationary Phases for μ-HPLC Separation of Peptides and Proteins. *Anal. Chem.* **2006**, *78* (14), 4969−4975.
(67) Gao, X.; Guo, C.; Hao, J.; Zhao, Z.; Long, H.; Li, M. Adsorption of Heavy Metal Ions by Sodium Alginate Based Adsorbent-a Review and New Perspectives. *Int. J. Biol. Macromol.* **2020**, *164*, 4423−4434.
(68) Zhang, S.; Wan, Y.; Yuan, W.; Zhang, Y.; Zhou, Z.; Zhang, M.; Wang, L.; Wang, R. Preparation of PVA−CS/SA−Ca2+ Hydrogel with Core−Shell Structure. *Polymers* **2022**, *14* (1), No. 212, DOI: 10.3390/polym14010212.
(69) Xia, Y.; Whitesides, G. M. Soft Lithography. *Angew. Chem., Int. Ed.* **1998**, *37* (5), 550−575.
(70) Zhang, L.; Chen, K.; Zhang, H.; Pang, B.; Choi, C. H.; Mao, A. S.; Liao, H.; Utech, S.; Mooney, D. J.; Wang, H.; Weitz, D. A. Microfluidic Templated Multicompartment Microgels for 3D Encapsulation and Pairing of Single Cells. *Small* **2018**, *14* (9), No. 1702955.
(71) Song, Y.; Kumar, C. S.; Hormes, J. Synthesis of Palladium Nanoparticles Using a Continuous Flow Polymeric Micro Reactor. *J. Nanosci. Nanotechnol.* **2004**, *4* (7), 788−793.
(72) Liu, R.; Wu, Q.; Huang, X.; Zhao, X.; Chen, X.; Chen, Y.; Weitz, D. A.; Song, Y. Synthesis of Nanomedicine Hydrogel Microcapsules by Droplet Microfluidic Process and Their PH and Temperature Dependent Release. *RSC Adv.* **2021**, *11* (60), 37814−37823.
(73) Wang, J.; Zhao, H.; Zhu, Y.; Song, Y. Shape-Controlled Synthesis of CdSe Nanocrystals via a Programmed Microfluidic Process. *J. Phys. Chem. C* **2017**, *121* (6), 3567−3572.
(74) Liu, W.; Zhang, Y. S.; Heinrich, M. A.; De-Ferrari, F.; Jang, H. L.; Bakht, S. M.; Alvarez, M. M.; Yang, J.; Li, Y. C.; Trujillo-de Santiago, G.; Miri, A. K.; Zhu, K.; Khoshakhlagh, P.; Prakash, G.; Cheng, H.; Guan, X.; Zhong, Z.; Ju, J.; Zhu, G. H.; Jin, X.; Shin, S. R.; Dokmeci, M. R.; Khademhosseini, A. Rapid Continuous Multimaterial Extrusion Bioprinting. *Adv. Mater.* **2017**, *29* (3), No. 1604630.
(75) Yin, J.; Yan, M.; Wang, Y.; Fu, J.; Suo, H. 3D Bioprinting of Low-Concentration Cell-Laden Gelatin Methacrylate (GelMA) Bioinks with a Two-Step Cross-Linking Strategy. *ACS Appl. Mater. Interfaces* **2018**, *10* (8), 6849−6857.
(76) Ying, G. L.; Jiang, N.; Maharjan, S.; Yin, Y. X.; Chai, R. R.; Cao, X.; Yang, J. Z.; Miri, A. K.; Hassan, S.; Zhang, Y. S. Aqueous Two-Phase Emulsion Bioink-Enabled 3D Bioprinting of Porous Hydrogels. *Adv. Mater.* **2018**, *30* (50), No. e1805460.
(77) Song, Y.; Sun, P.; Henry, L. L.; Sun, B. Mechanism for Structure and Performance Controlled Preparation of Thin Film Composite Membrane via Interfacial Polymerization. *Journal of Membrane Science* **2005**, *251* (1-2), 67−79.
(78) Song, Y.; Liu, F.; Sun, B. Preparation, characterization, and application of thin film composite nanofiltration membranes. *J. Appl. Polym. Sci.* **2005**, *95* (5), 1251−1261.
(79) Zhang, W.; Zhao, X.; Yuan, Y.; et al. Microfluidic Synthesis of Multimode Au@CoFeB-Rg3 Nanomedicines and Their Cytotoxicity and Anti-Tumor Effects. *Chem. Mater.* **2020**, *32* (12), 5044−5056.
(80) Zhao, X.; Wu, J.; Guo, D.; et al. Dynamic ginsenoside-sheltered nanocatalysts for safe ferroptosis-apoptosis combined therapy. *Acta Biomater.* **2022**, *151*, 549−560.

https://doi.org/10.1021/acs.langmuir.3c02579
Langmuir XXXX, XXX, XXX−XXX